

High-Throughput Screening of Cell Transfection Enhancers Using Miniaturized Droplet Microarrays

Yanxi Liu, Tina Tronser, Ravindra Peravali, Markus Reischl, and Pavel A. Levkin*

DNA delivery is a powerful research tool for biological research and clinical therapies. However, many nonviral transfection reagents have relatively low transfection efficiency. It is hypothesized that by treating cells with small molecules, the transfection efficiency can be improved. However, in order to identify such transfection-enhancing molecules, thousands of molecules must be tested. Current high-throughput screening (HTS) technologies based on microtiter plates are not suitable for such screenings due to the prohibitively high costs of reagents and operation. Here, the use of the droplet microarray (DMA) platform to screen 774 FDA-approved drugs with CHO-K1, Jurkat and HEK293T cells is reported. The volume of individual aqueous compartments is 20 nL, requiring 0.84 mL of cell suspension and 200 pmoles of each drug (total 0.02 moles) to perform the screening. Thus, the requirement for cells and reagents is 2500 times less than that for the same experiment performed in 384-well plates. The results reveal the potential of the DMA platform as a more cost-effective and less labor-intensive approach to HTS. Furthermore, an increase (approximately two- to fivefold) in transfection efficiency is achieved by treating cells with some molecules. This study clearly demonstrates the potential of the DMA platform for miniaturization of biochemical and cellular HTS.

gene disorders, infection, and cancers.^[5] However, many nonviral transfection reagents have relatively low transfection efficiency as they are usually hindered by numerous extra- and intracellular obstacles.^[6] Many researchers focused on this field and developed various gene delivery vehicles to achieve safe, efficient, and controllable gene delivery, including biodegradable nanoparticles,^[7] polymer-based gene delivery systems,^[8] stimuli-responsive nanocarriers,^[9] lipid-based vectors,^[10] and polypeptides-based vectors.^[11] Although these methods have advantages in terms of nonimmunogenicity and nononcogenicity of vectors, most of these approaches suffer from poor efficiency of delivery and transient expression of the gene. In addition, one of the drawbacks of these approaches is the diminished specificity of these materials.^[12] A lot of the current gene-therapy approaches make use of viral vectors. Nevertheless, humans have an immune system to fight off the virus, resulting in the safety concerns of viral gene delivery.^[3b]

1. Introduction

Over the past 30 years, large significant efforts have been dedicated to develop nanotechnology by which various molecules or macromolecules, such as proteins,^[1] peptides,^[2] and genes^[3] can be successfully targeted to sites of interests. DNA delivery, especially via the nonviral route (i.e., gene transfection), has become a powerful research tool for elucidating gene structure, regulation, and function.^[4] DNA delivery has been pivotal in developing new approaches (e.g., gene therapy and DNA vaccination) for biological research and new clinical therapies. Gene therapy provides a great opportunity to treat diseases from

In vivo and in vitro gene delivery has also been traditionally hindered by the toxicity associated with their formulation.^[13]

In 1983, Luthman et al. reported that exposure to chloroquine increased the proportion of transfected mouse cells to $\approx 40\%$.^[14] Afterward, several researchers reported neomycin,^[15] dexamethasone,^[16] and nocodazole^[17] also made a contribution to the transfection efficiency enhancement. Hence, in the present project, we hypothesized that by treating cells with small molecules, the transfection efficiency can be improved in a safe and controllable way. Nevertheless, in order to identify such transfection-enhancing molecules, thousands of structurally diverse molecules must be tested. Current high-throughput screening (HTS) technologies

Y. Liu, Dr. T. Tronser, Dr. R. Peravali, Dr. P. A. Levkin
Institute of Toxicology and Genetics (ITG)
Karlsruhe Institute of Technology (KIT)
Hermann-von Helmholtz-Platz 1
Eggenstein-Leopoldshafen 76344, Germany
E-mail: pavel.levkin@kit.edu

 The ORCID identification number(s) for the author(s) of this article can be found under <https://doi.org/10.1002/adbi.201900257>.

© 2020 The Authors. Published by WILEY-VCH Verlag GmbH & Co. KGaA, Weinheim. This is an open access article under the terms of the Creative Commons Attribution-NonCommercial License, which permits use, distribution and reproduction in any medium, provided the original work is properly cited and is not used for commercial purposes.

Dr. M. Reischl
Institute for Automation and Applied Informatics (IAI)
Karlsruhe Institute of Technology (KIT)
Hermann-von Helmholtz-Platz 1
Eggenstein-Leopoldshafen 76344, Germany
Dr. P. A. Levkin
Institute of Organic Chemistry
Karlsruhe Institute of Technology (KIT)
Fritz-Haber-Weg 6, Karlsruhe 76131, Germany

DOI: 10.1002/adbi.201900257

based on microtiter plates cannot be used in such screenings due to prohibitively high costs associated with large volumes of reagent and the man-power required.^[18]

In the last decades, a great deal of effort has been made to develop innovative miniaturized platform for biological screening, including inkjet printing,^[19] microfluidic technology,^[20] cell-based microarrays,^[21] and nanowell array chip.^[22] The chip array based on inkjet printing technique can be used to develop up to hundreds of picoliter aqueous droplet arrays and can be further applied to do biological assays, such as luminometric detection and protein binding assays.^[19] However, the compatibility of cells within such a tiny volume need to be further investigated and the employment of oil phase might influence its application with cells. The microfluidic-based chip and nanowell array chip could be used to establish 2D or 3D *in vitro* cell culture model systems for cell cytotoxicity screening and real-time drug delivery monitoring.^[20,22] Nevertheless, the involvement of oil phase might restrict its applicability and high-throughput applications. Cell-based microarrays introduced by Sabatini allow high-throughput screening in a highly miniaturized format.^[21] However, the transfection mixtures need to be preprinted onto the glass slides or arrays, and the slides have to be immersed into one medium, which means they cannot have separate compartments after cell seeding. The small drug molecules can freely diffuse within the medium, resulting in cross-contamination.

Our group has recently developed the droplet microarray (DMA) platform based on the superhydrophobic–hydrophilic surfaces,^[23] which can be applied to high-throughput screenings of live cells in 2D and 3D,^[24] including cytotoxicity screening, embryoid bodies screening, tumor spheroids screening, and zebra fish embryo screening. However, such large screening (41796 individual experiments) with extremely small volumes (20 nL) has never been done so far. This ultrahigh throughput and miniaturization impose completely new challenges to the droplet microarray platform, which we aimed to investigate in this work using cell transfection as a crucial biological tool used in drug discovery and related fields. High-density arrays of nanoliter sized droplets with defined shapes could be formed on this superhydrophobic–hydrophilic transparent layer on the glass slide. The DMA platform has the following advantages: a) three orders of magnitude less cells and reagents; b) compatibility with cells in different characteristics, such as adherent and suspension cells; c) avoid cross-contamination combining with the noncontact printer; d) less pipetting manipulation; and e) applicability to ultrahigh-throughput screening. Furthermore, the drugs can be dried on each individual spots for multiple detection for different read-out which makes the DMA platform more flexible for multiple applications. The separate individual spots also raise the possibility to repeatedly add solutions or cells without any cross-contamination since the liquid can be printed precisely into each individual spot. By adjusting the size of spots, a higher-throughput can also be achieved. Compared to conventional experiments conducted in microtiter plates, such as 384- and 96-well plates, screening on our DMA could lead to around 2500-fold costs saving compared to experiments conducted in 384-well plates.

In this study, we investigated the influence of 774 Food and Drug Administration (FDA)-approved drugs on transfection efficiency with CHO-K1, Jurkat and HEK293T cells. We performed a screening of the drugs using the DMA platform in

three concentrations with triplicates based on two cell lines and repeated three times, resulting in a total of 41 796 individual experiments. The volume of individual aqueous compartments was 20 nL, requiring only 0.84 mL of total cell suspension and 200 pmoles of each drug (total 0.02 moles) to perform the screening. Thus, the requirement for the cells and reagents was 2500 times less than that for the same experiment performed in 384-well plates. The results reveal the potential of the DMA platform as a more cost-effective and less labor-intensive approach to HTS, making this technology a viable option in a standard biology laboratory. Furthermore, we achieved an increase (approximately 2-5-fold) in transfection efficiency by treatment of the cells with some small molecules (auranofin, carbidopa, captopril, hydrocortisone acetate, ifosfamide, indapamide, oxacillin sodium salt monohydrate, methylprednisolone, naphazoline·HCl, rifampin, oxiconazole nitrate, piroxicam, tranlycypromine hemisulfate and rivastigmine tartrate) approved for other indications. This was confirmed in standard transfection experiments in 384- and 96-well plates with CHO-K1 and HEK293T cells. This study clearly demonstrates the potential of the DMA platform for miniaturization of biochemical and cellular HTS.

2. Results and Discussion

2.1. Establishment of an HTS Assay for CHO-K1 and Jurkat Cells

DMA slide is a glass slide patterned with an array of hydrophilic spots assigned by superhydrophobic borders based on certain substrate. We used different DMA slides with a dimension of 7.5 × 2.5 cm divided into three square fields (left field, center field, and right field) containing 588 (1 mm side length of square spots) and 2187 (500 μm side length of square spots) individual spots (Figure 1A; and Figure S1, Supporting Information). Because of the precise patterned square spots and stable borders, homogeneous cellular microarrays can be created by printing cell suspensions directly into each individual spot using a noncontact cell printer and further incubated for determined time (Figure 1B). The efficiency of transfection can be analyzed using regular fluorescence microscopy (Figure 1C). Beyond that, this system is also accessible for culturing and transfecting cells with different characteristics, such as adherent and suspension cells (Figure 1D–F).

In order to identify drug candidates that can potentially enhance transfection efficiency and/or increase the numbers of green fluorescent protein (GFP)-expressing cells, we developed an HTS assay that can rapidly screen numerous compounds. As for cell systems, we chose CHO-K1 cells, Jurkat, and HEK293T cells. CHO-K1 cells are one of the most important cell lines for the production of biotherapeutic protein and antibodies, but they are typically difficult to transfect. Jurkat cells are an immortalized line of human T lymphocyte which are widely used due to their relevance to blood cells. And HEK293T cells are a standard cell line used by many scientists because of their propensity for transfection.

A schematic of the HTS workflow is depicted in Figure 2; and Figure S2 (Supporting Information). In the first step, the stock solution of 774 FDA-approved drugs were diluted to three concentrations 1, 10, and 30 × 10⁻⁶ M, and then 20 nL of each

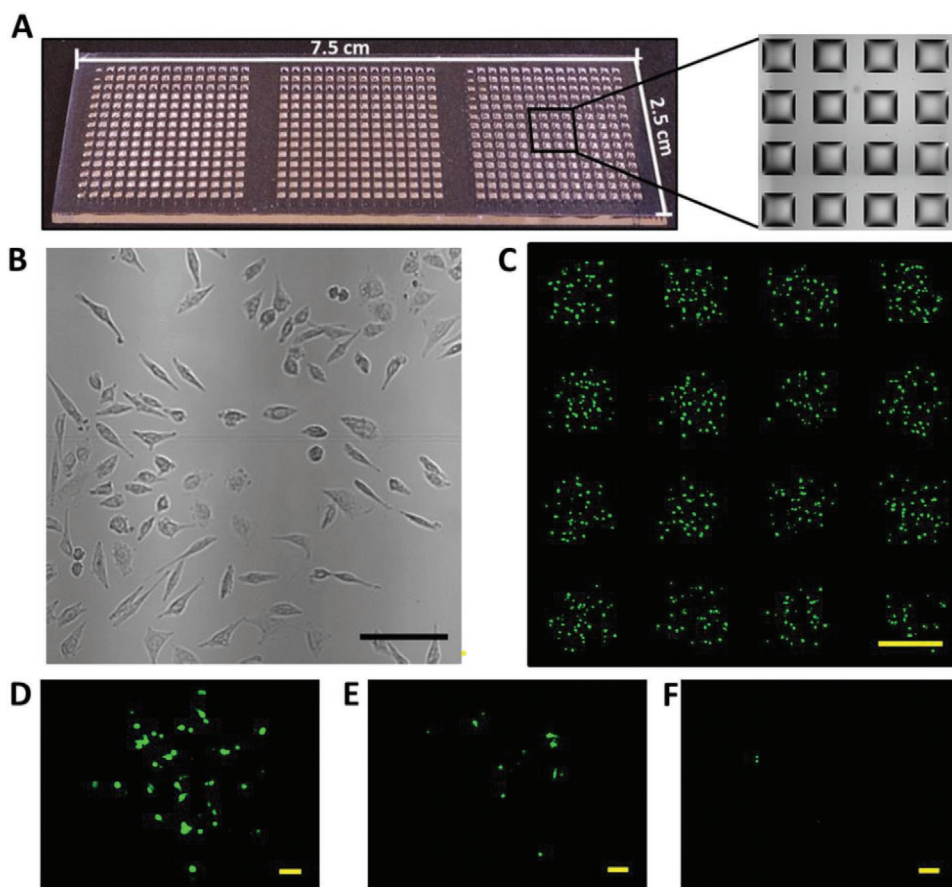


Figure 1. A) Representative image of 1 mm (square side length is 1 mm) droplet microarray (DMA) with 588 individual microdroplets. Size of the DMA slide is 7.5 ± 2.5 cm. B) Bright field microscope image showing morphology of CHO-K1 cells after 24 h incubation (scale bar: 100 μ m). C) Representative image of HEK293T cells transfected with GFP plasmid DNA on the droplet microarray with 1 mm spot size (scale bar: 1 mm). Fluorescence microscope images of individual microdroplets of D) HEK293T cells, E) CHO-K1 cells, and F) Jurkat suspension cells transfected with GFP plasmid DNA (scale bar: 100 μ m).

drug was printed on 500 μ m DMA slides. After drug printing, certain amount of dimethyl sulfoxide (DMSO) were still in each spot, which was toxic for the cells. To remove DMSO from the spots and to make all the conditions the same during printing, the slides were dried in a vacuum desiccator overnight. Complexes of GFP plasmid DNA and ScreenFectA transfection reagent were prepared and then printed into each spot and incubated with drugs at three concentrations along with a drug-free control (DMSO). And the same three controls were located at each square field inside of each slide. Besides, the outer two rows and columns were subtracted because of the edge effect. After 24 h incubation, cells were fixed, and the GFP expressed cells were imaged by an automated fluorescence microscope and the number of GFP-positive cells was quantified. Then the relative transfection enhancement was calculated as a ratio of the mean number of GFP positive cells for each drug over the mean number of GFP positive cells of drug-free controls. Heat-maps in **Figure 3A** demonstrate the result of primary screening of CHO-K1 cells. The blue cells of the heatmap represent wells with less GFP positive cells than that in the drug-free control wells, while the red color represents experiments with more GFP positive cells than that in the drug-free controls. For CHO-K1 cells, there were 425 compounds which showed transfection

enhancement, while 349 compounds showed transfection decrease at the concentration of 1×10^{-6} M when compared to drug-free controls. As for 10×10^{-6} M, 624 compounds showed transfection enhancement while 150 compounds showed transfection decrease. At 30×10^{-6} M, the numbers of the transfection enhancement and transfection decrease were 233 and 541, respectively. The transfection enhancement demonstrated a concentration-dependent manner and at the concentration of 10×10^{-6} M, the most drugs showed transfection enhancement compared to the concentration of 1 and 30×10^{-6} M. It might be that the drugs have various influence on the cellular endocytosis, intracellular delivery and localization of the transfection complex, resulting in a different expression of GFP followed by different transfection efficiency. Primary hits (hit compounds) were identified as drugs that increased the number of GFP positive cells in comparison to the drug-free mean by at least three standard deviations. Thus, at 1×10^{-6} M concentration, 19 hits were identified, as well as 78 hits at 10×10^{-6} M concentration and 18 hits at 30×10^{-6} M concentration (**Figure 4**). Seven compounds (auranofin, captopril, tranlylcypromine hemisulfate, piroxicam, carbidopa, oxacillin sodium salt monohydrate, and oxiconazole nitrate) showed repeatable transfection enhancement at different concentrations. There are more

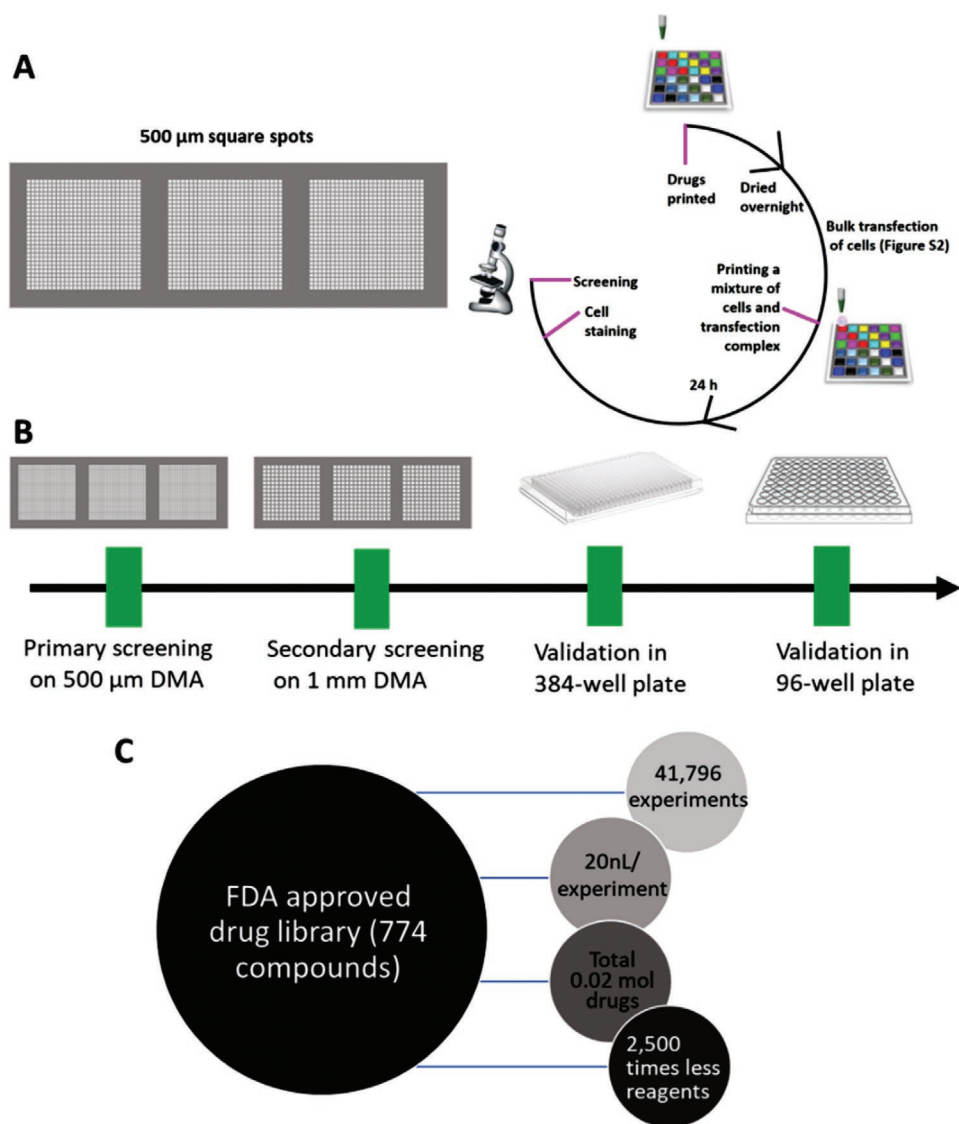


Figure 2. The workflow of the primary cell screening. A) 774 FDA approved drugs as DMSO solutions were printed on 500 μm DMA slides and dried in the vacuum desiccator overnight. Cells mixed with the transfection mixture (ScreenFectA transfection reagent, GFP plasmid DNA) were then printed into each spot and incubated with drugs for 24 h before fixation and fluorescence microscopy analysis. Final concentrations of drugs in the were 1, 10, and 30×10^{-6} M. 14 hit compounds from primary screening were printed onto the 1 mm DMA slides and the procedure was repeated in the same way, except for the use of larger concentration ranges: 1, 5, 10, 20, 30, and 40×10^{-6} M. For the drug-free control experiments, the transfection mixtures were printed into empty spots. B) The process of high-throughput screening designed for transfection enhancers screening. The primary screening was conducted on 500 μm DMA slides (20 nL per experiment) and the secondary screening was done on 1 mm DMA slides (100 nL per experiment). Further validation and comparison was carried out in conventional high-throughput screening platform 384-well plates. Finally, the hits were confirmed in 96-well plates under optimized conditions. C) Screening of 774 FDA-approved drugs in three concentrations, resulted in a total of 41 796 individual experiments. The volume of individual aqueous compartments was 20 nL, which in total resulted in only 0.84 mL of total cell suspension and require only 200 pmoles of drugs (total 0.02 moles), which is 2500 times smaller than if the same experiment would have to be performed in 384-well plates.

hits at 10×10^{-6} M than at 1×10^{-6} M, it might be the stimuli from the drugs at low concentration increases the cell division activity which could lead to the negative results. There are more hits at 10×10^{-6} M concentration than at 30×10^{-6} M, which can be explained by increased toxicity at the highest concentration used and, thus lower overall cell number per experiment.

Furthermore, a principal component analysis (PCA) based multiobjective optimization procedure was also utilized for double verification of the screening results to get rid of false

signals and for the dimensionality reduction, whose efficacy was demonstrated by solving up to 50-objective optimization problems.^[25] In the PCA score plot (Figure 3B), each number represented one drug and significantly different behaviors of transfection under different drugs can be observed. The GFP expressed cell numbers vary in the presence of drugs, resulted in drugs that were distinct from the transfection under control conditions. The outliers (hit compounds) got from the PCA analysis are almost the same as identified using the above algorithm.

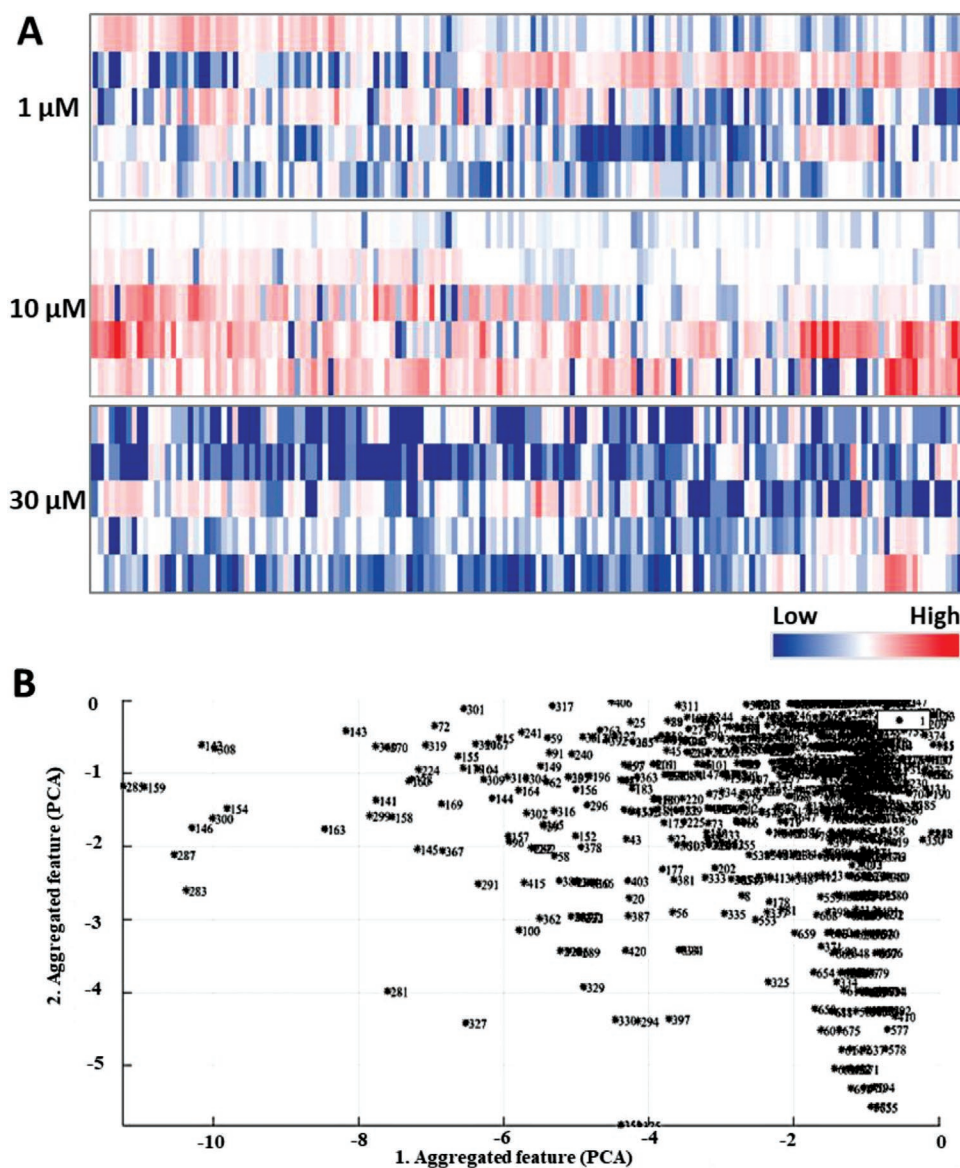


Figure 3. The impact of FDA-approved drugs on the efficiency of transfection of CHO-K1 cells. A) Heat maps generated using the quantified relative transfection efficiency data from 20 898 total transfection experiment (three biological repeats and three replicates each time). The blue and red colors indicate either decrease or increase of efficiency, respectively, in comparison to the controls without addition of drugs. Three different drug concentrations were used: 1, 10, and 30×10^{-6} M. B) Overview of primary screening results using the principal component analysis (PCA) score plot. Each number represents one drug from the FDA-approved drug library.

The same primary screening was also conducted with Jurkat human T-cell lymphocyte cells, which has traditionally proven to be very difficult to transfect due to a reduced attachment of the transfection complex to the surface of cells.^[26] The results of the primary screening of Jurkat cells showed significantly less positive hits in comparison to the transfection of CHO-K1 cells (Figure S5 and Table S1, Supporting Information). For Jurkat cells, there were 244 compounds which showed transfection enhancement while 530 compounds showed transfection decrease at the concentration of 1×10^{-6} M when compared to the drug-free controls. As for 10×10^{-6} M, 325 compounds showed transfection enhancement while 449 compounds showed

transfection decrease. At 30×10^{-6} M, the numbers of the transfection enhancement and transfection decrease were 192 and 582, respectively. Due to the difficult transfection characteristic of Jurkat cells, less transfection enhancement compounds could be found compared to CHO-K1 cells. When the threshold of the primary screening was set as mean + 3SD, no hits were identified at 1×10^{-6} M concentration. But 2 hits at 10×10^{-6} M concentration and 1 hit at 30×10^{-6} M concentration were identified (Figure S5 and Table S1, Supporting Information). The higher overall transfected cell number demonstrates six- to eightfold relative transfection enhancement of the two hits compared to the drug-free controls in the primary screening.

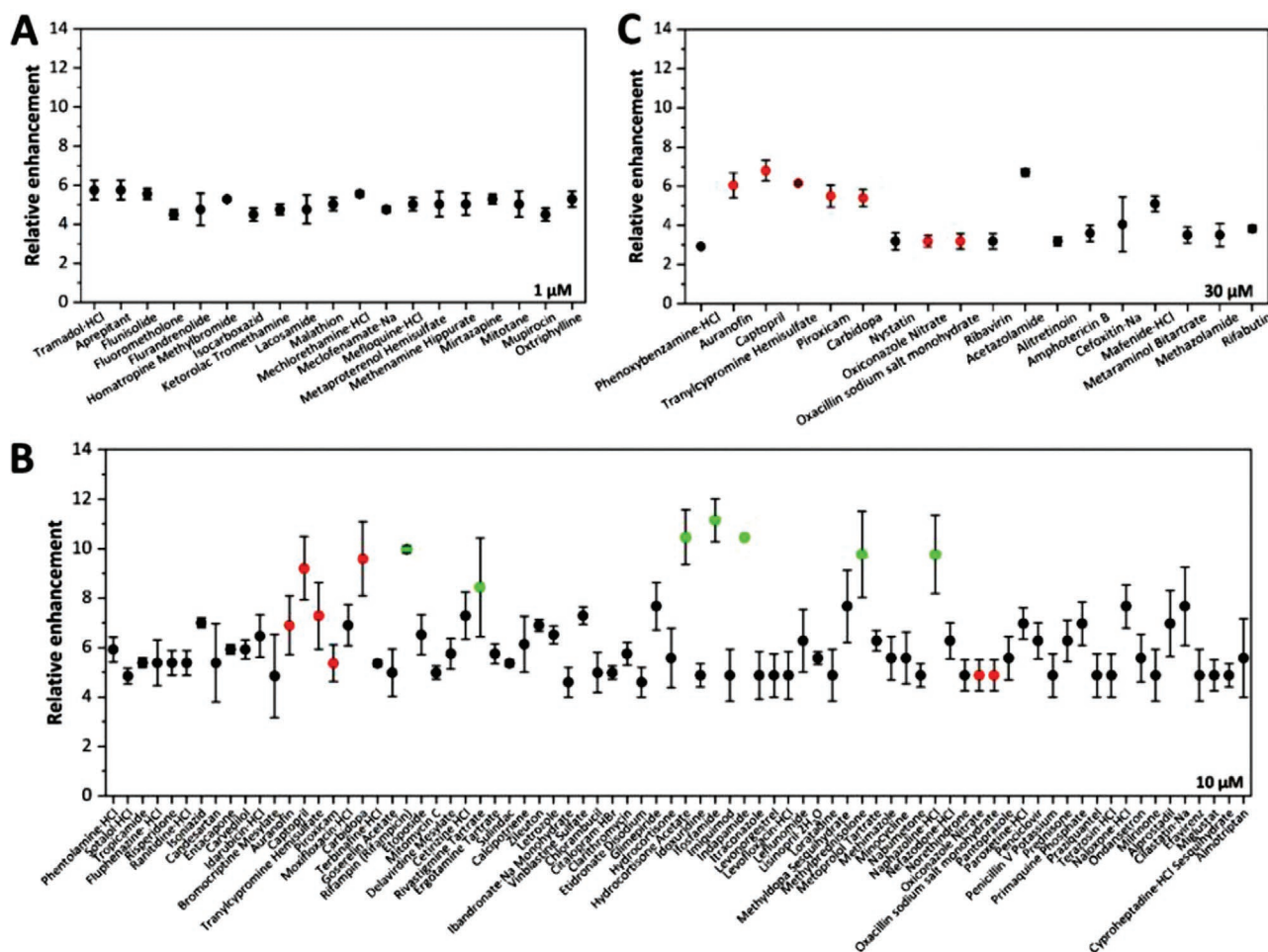


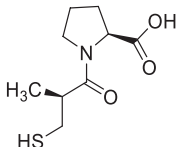
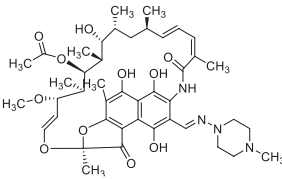
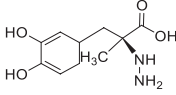
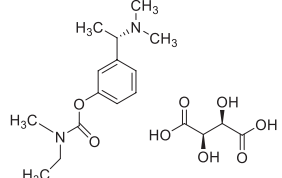
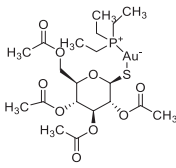
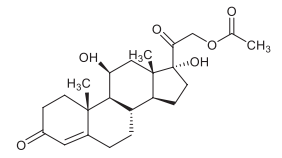
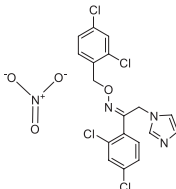
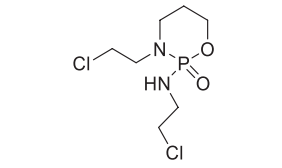
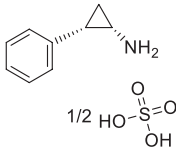
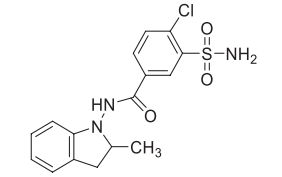
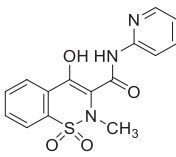
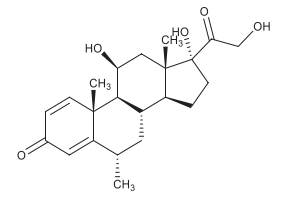
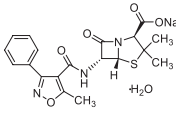
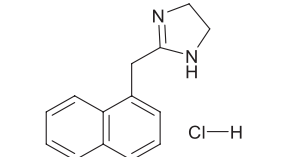
Figure 4. Hit compounds identified as transfection enhancers in the primary screening of CHO-K1 cells. A) 19 out of 774 FDA-approved drugs obtained from primary screening at 1×10^{-6} M concentration of CHO-K1 cells. B) 78 hit compounds identified at 10×10^{-6} M concentration. C) Scatter plot of 18 hit compounds obtained from primary screening at 30×10^{-6} M of CHO-K1 cells. The red color indicated the compounds (auranofin, captopril, tranylcypromine hemisulfate, piroxicam, carbidopa, oxacillin sodium salt monohydrate, and oxiconazole nitrate) that showed repeatable positive enhancement at different concentrations and the green color indicated the compounds (rifampin, rivastigmine tartrate, hydrocortisone acetate, ifosfamide, indapamide, methylprednisolone, and naphazoline-HCl) that showed strong enhancement effect at one concentration. Data were presented as mean \pm SD of three biological experiments with three technical repeats each time.

2.2. Validation of Primary Hits as Transfection Enhancers

In the primary screening, we assumed that the numbers of cells printed onto each individual spot are the same. Nevertheless, cells will precipitate during printing due to the printing pressure and gravity, resulting in the variability of cell numbers among spots (Figure S3, Supporting Information). For this reason, the hits from the primary screening were further validated. We selected 14 compounds that showed a strong enhancement effect at one concentration or showed repeatable positive enhancement at different concentrations for the secondary screening in order to validate the observed effects (Table 1; and Figure S4, Supporting Information). The validation experiment was performed in the 1 mm DMA (Figure 2B) at concentrations ranging from 1 to 40×10^{-6} M. To further test whether the transfection hits help in transfection efficiency enhancement, we introduced HEK293T, which is a well-known easy to transfect cell type,^[27] to test the hits from the primary

screening as well. Each drug was evaluated by three parameters: 1) number of GFP expressing cells, 2) dead cell number (stained by PI), and 3) total cell numbers (stained by Hoechst 33342). Figure 5 demonstrates the transfection efficiency and cell viability for each drug. The secondary screening showed obvious and reproducible dose-dependent effects of the drugs on transfection efficiency. Transfection efficiencies increased between 1.8-fold to 5.1-fold compared to drug-free control. However, 12 out of 14 hits showed considerable transfection efficiency reduction at higher drug concentrations due to the high toxicity toward cells (30 and 40×10^{-6} M). In the case of piroxicam and tranylcypromine hemisulfate, the transfection enhancement is observed even at higher concentrations. Some drugs (ifosfamide, methylprednisolone, and oxacillin sodium salt monohydrate) showed the same trend in the primary screening and the secondary screening. All 14 compounds also demonstrated a dose-dependent negative effect on cell viability of CHO-K1 cells.

Table 1. 14 Hit compounds selected from the primary screening.

Compound	Therapeutic effect	Structure	Compound	Therapeutic effect	Structure
Captopril	Inhibitor of angiotensin-converting enzyme (ACE)		Rifampin (Rifampicin)	Inhibitor of DNA-dependent RNA polymerase	
Carbidopa	Inhibitor of DOPA decarboxylase		Rivastigmine tartrate	Inhibitor of parasympathomimetic and cholinesterase	
Auranofin	Inhibitor of kappaB kinase and thioredoxin reductase		Hydrocortisone acetate	Antiinflammatory or immunosuppressive drug	
Oxiconazole nitrate	Antibiotic used in resistant staphylococci infections		Ifosfamide	Alkylating agent and immunosuppressive agent	
Tranlycypromine hemisulfate	Inhibitor of monoamine oxidase (MAO)		Indapamide	Antihypertensive and diuretic agent	
Piroxicam	Inhibitor of cyclooxygenase, nonsteroidal antiinflammatory agent (NSAID)		Methylprednisolone	Antiinflammatory and immunosuppressive agent	
Oxacillin sodium salt monohydrate	Penicillin beta-lactam antibiotic		Naphazoline-HCl	Sympathomimetic alpha adrenergic agonist	

The hits validation with Jurkat cells (Figure S6, Supporting Information) and HEK293T cells (Figure S7, Supporting Information) are also presented. The results of HEK293T that is a well-known easy to cultivate and transfect cell type, also showed the same transfection efficiency enhancement trend as CHO-K1 cells with higher absolute transfection efficiency (between 1.2-fold to 3.5-fold increase compared to drug-free control). In the case of Jurkat cells, no significant transfection enhancement

was observed at all concentrations tested, probably due to the overall too low transfection efficiencies.

In order to further validate the obtained results, we compared the transfection efficiency of hits at their optimum concentrations on DMA (Table S2, Supporting Information) on both DMA slides and conventional 384-well plates of CHO-K1 cells (Figure 6) and HEK293T cells (Figure S8, Supporting Information). In general, the transfection efficiency

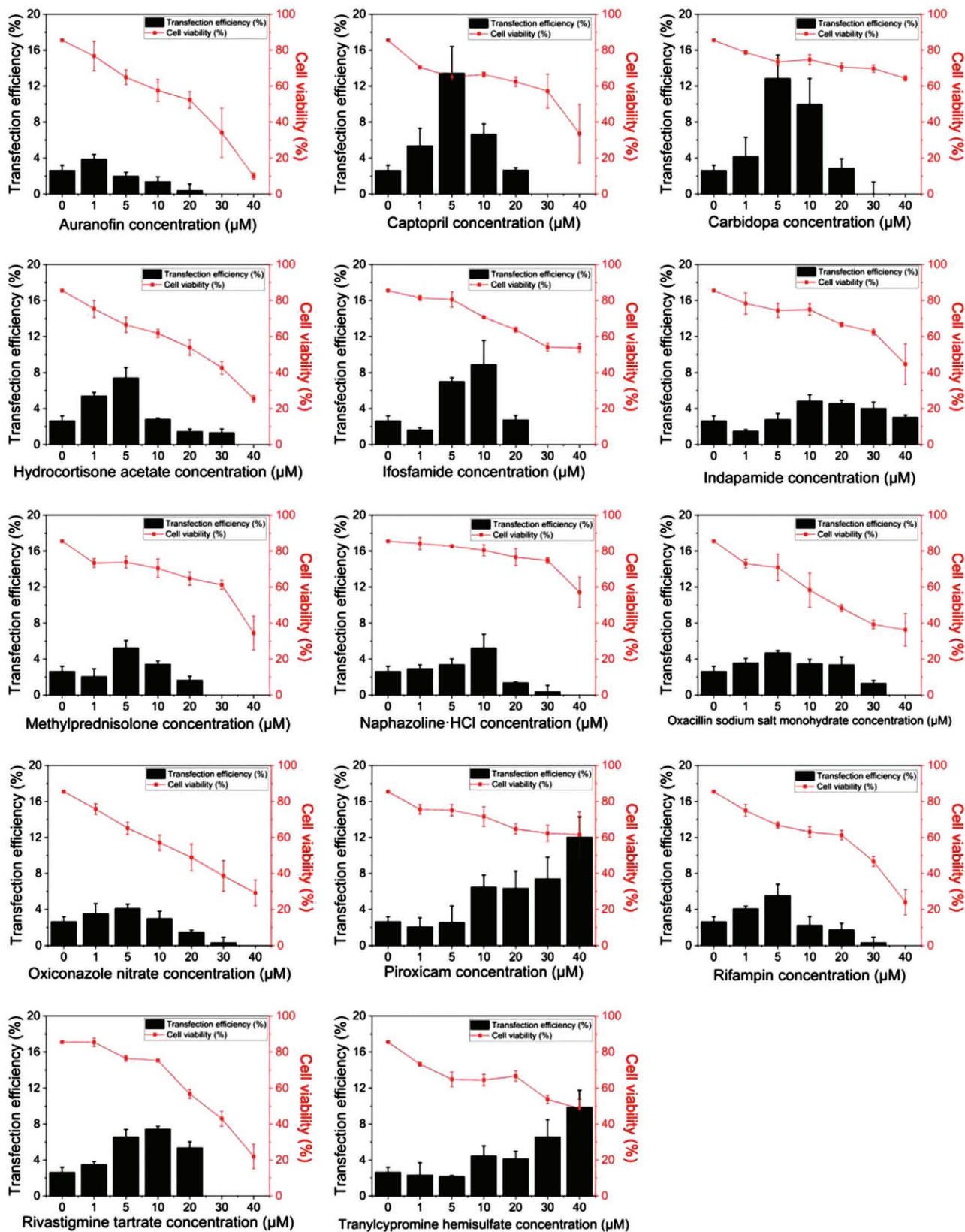


Figure 5. Impact of 14 hit compounds on GFP plasmid DNA transfection of CHO-K1 cells. Different amounts of fourteen hit compounds (auranofin, carbidopa, captopril, hydrocortisone acetate, ifosfamide, indapamide, oxacillin sodium salt monohydrate, methylprednisolone, naphazoline-HCl, rifampin, oxiconazole nitrate, piroxicam, tranlycypromine hemisulfate, and rivastigmine tartrate) were printed onto 1 mm DMA, dried in the vacuum

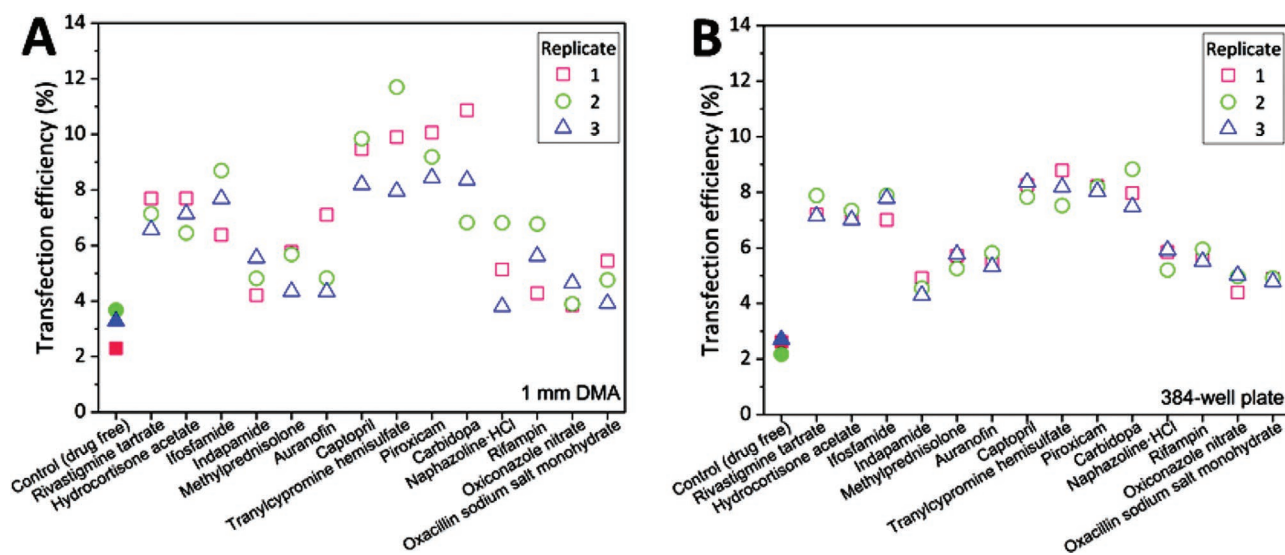


Figure 6. The impact of hit compounds from primary screening under the best concentration in the individual spots on A) 1 mm DMA and in B) 384-well plates of CHO-K1 cells in all three analyzed replicates in both formats. Transfection efficiency in every image taken/per well (per spot) is shown separately. The different shapes indicate individual replicates (replicate 1-square, replicate 2-circle, and replicate 3-triangle). The optimal working concentrations of each drug according to the secondary screening were used for each drug (Table S2, Supporting Information). The transfection complexes were prepared with 0.017 μL ScreenFectA in 10 μL ScreenFect dilution buffer, followed by diluting a total of 17 ng GFP plasmid DNA in dilution buffer to a final volume of 10 μL (ratio of the ScreenFectA-to-plasmid DNA is 1:1). Then 80 μL fresh cell suspension at a concentration of 7.13×10^4 cells mL^{-1} were added to complexes followed by mixing and seeding into each well at a volume of 20 μL per well. Data were presented as mean \pm SD of three biological experiments with three technical repeats each time.

of the individual wells in 384-well plates was less variable than that on the individual spots on DMA, which can be attributed to the 11.35-fold less cells in each droplet of the DMA in comparison with the plate format (100 nL per spot and 100 cells per spot vs 20 μL per well and 1135 cells per well). While the average transfection efficiency showed no significant differences between the two platforms, confirming the validity of the results from the primary and secondary screening and the possibility to translate obtained results into larger, more commonly used formats, such as microtiter plates.

2.3. Validation of the Results under Optimal Conditions

Since DMA and conventional microtiter plates are two different in vitro cell culture systems in terms of the cell cultivation and experiment parameters might be diverse due to the discrepancy in formats, edge-effects, evaporation, and area to volume ratio. The transfection parameters are also supposed to be different. Therefore, we selected four hits (hydrocortisone acetate, naphazoline·HCl, oxacillin sodium salt

monohydrate, and piroxicam) after validation and further evaluated the transfection efficiency in an optimal condition of transfection in 96-well plates. First, the transfection optimization in the presence or absence of the drugs was conducted according to the manufacturer's instruction (Figure S9A–E, Supporting Information) using transfection reagent amounts from 0.1 to 0.4 $\mu\text{L}/96$ -well plate well and from 50 to 100 ng per well of plasmid DNA. As shown in Figure S9 (Supporting Information), the highest transfection efficiency was achieved at 0.4 μL transfection reagent with 100 ng DNA per well with or without the drugs. Thus, these conditions were chosen for the following experiments. The transfection efficiency and cell viability were evaluated with these four drugs and compared with the drug-free control. As shown in Figure S9F (Supporting Information), naphazoline·HCl, oxacillin sodium salt monohydrate, and piroxicam could increase the transfection efficiency from $30.3\% \pm 1.6\%$ (drug-free control) to $36.3\% \pm 0.9\%$, $38.8\% \pm 1.1\%$, $33.9\% \pm 1.2\%$, respectively. It should be noted that the mechanisms behind the increase of transfection efficiency caused by these molecules are still unknown and need further investigation. The transfection enhancement may be caused by the influence of these drugs on the expression of

desiccator overnight, followed by printing pretransfected cells and incubation for 24 h in 100 nL droplets before quantification. Treatments were performed at concentrations of 0, 1, 5, 10, 20, 30, and 40×10^{-6} M for each compound. After that, cells on DMA were stained with Hoechst 33 342 to visualize cell nuclei and propidium iodide (PI) to distinguish dead cells. DMA was then placed in a petri cell culture incubator for 15 min. Fluorescence images were taken using the Olympus IX81 inverted motorized microscope. The number of GFP positive, Hoechst 33 342 and PI-positive cells were counted using Image J. Cell viability was calculated using the following equation: cell viability (%) = $1 - (\text{PI-positive cell numbers}/\text{Hoechst positive cell numbers}) \times 100$. The transfection efficiency was calculated as follows: transfection efficiency (%) = $(\text{GFP positive cell numbers}/\text{Hoechst positive cell numbers}) \times 100$. Data were presented as mean \pm SD of three biological experiments with ten technical repeats each time.

particular genes involved in the cellular uptake processes, endosomal escape, or other mechanisms.^[28] The results of this study demonstrate the great potential of the DMA platform in miniaturized high-throughput drug screenings, high-throughput cell transfection experiments, and search for new biologically active molecules.

3. Conclusion

In this study, we systematically screened the effect of 774 FDA-approved drugs and their concentrations on transfection efficiency in three different cell types. Based on the primary screening, 14 hit compounds were selected and further evaluated and validated on the droplet microarray platform as well as both in 384- and 96-well plates. Several compounds (auranofin, carbidopa, captopril, hydrocortisone acetate, ifosfamide, indapamide, oxacillin sodium salt monohydrate, methylprednisolone, naphazoline·HCl, rifampin, oxiconazole nitrate, piroxicam, tranlycypromine hemisulfate, and rivastigmine tartrate) showed up to fivefold increase of transfection efficiency, which can be important for the fundamental research projects but also for the production of therapeutically relevant proteins. Our results also demonstrate the power of the droplet microarray platform in miniaturized high-throughput experiments. In this study, we performed in total around 42 000 individual experiments using 20 nL droplets, which resulted in only 0.84 mL of total cell suspension and required only 200 pmoles of drugs (total 0.02 moles). This is 2500 times smaller than if the same experiment would have to be performed in 384-well plates (Figure 2C).

4. Experimental Section

Materials: Formaldehyde solution, Thermo Scientific Shandon Immount, Hoechst 33 342 (1.0 mg mL⁻¹ in water) and propidium iodide (PI, 1.0 mg mL⁻¹ in water) were purchased from Thermo Fisher Scientific Inc. (MA, USA). ScreenFectA transfection reagent was obtained from ScreenFect (Eggenstein-Leopoldshafen, Germany). Fetal calf serum (FCS), RPMI-1640 cell culture medium, 0.25% trypsin/EDTA, Dulbecco's Modified Eagle's Medium (DMEM), 1% penicillin/streptomycin solution were purchased from Gibco, Life Technologies GmbH (Darmstadt, Germany). Ham's F12 medium was purchased from Biowest (Nuaillé, France).

Droplet Microarray: The DMA slides were purchased from Aquarray (Aquarray, Eggenstein-Leopoldshafen, Germany) and they were sterilized in absolute ethanol for 60 min ensuing drying on the cell culture bench before using.

Cell Culture: Jurkat human T-cell lymphocyte cells were maintained in RPMI-1640 cell culture medium supplemented with 10% heat-inactivated FCS and 1% penicillin/streptomycin at 37 °C in a 5% CO₂ incubator. Chinese hamster ovary CHO-K1 cells were cultured in Ham's F12 medium supplemented with 10% FCS at 37 °C in a 5% CO₂ humidified atmosphere. Cells were trypsinized using 0.25% trypsin/EDTA and were regularly split to keep them in the logarithmic phase of growth. Human embryonic kidney 293T (HEK293T) cells were cultured in complete DMEM supplemented with 10% fetal calf serum at 37 °C in a 5% CO₂ humidified incubator. Cells were trypsinized using 0.25% trypsin/EDTA and were regularly split to keep them in the logarithmic phase of growth.

GFP Plasmid DNA Preparation: A plasmid encoding for green fluorescent protein (pGFP) was used as a reporter gene to monitor

the results of gene transfection. Highly purified covalently closed circular plasmid DNA was isolated by plasmid purification mini and maxi kits from Qiagen (Valencia, CA) according to the manufacturer's instructions. The final concentration of DNA was 0.5–2.0 µg µL⁻¹ and the A₂₆₀/A₂₈₀ value was above 1.8. Prepared plasmid DNA was stored at –20 °C for further using.

Drug Library: The Screen-Well FDA-approved drug library V2, consisting of 774 compounds, was provided as 10 × 10⁻³ M stock solutions in dimethyl sulfoxide (BML-2843 Version 1.2; Enzo Life Sciences, Albany, NY, USA) and arrayed in a total 11 96-well plate, leaving the first and last columns in each plate for controls. Each drug solution in these microplates was diluted with sterile water to produce 100 × 10⁻⁶ M prediluted plates. The prediluted drug plates were sealed and stored at –80 °C.

Printing: FDA-approved drug library was preprinted into each spot on DMA at various concentrations and volumes using sciFLEXARRAYER S11 dispenser (Scienion AG, Berlin, Germany) followed by drying in a desiccator under 50 mbar vacuum overnight. Since small volumes (2 nL for 1 × 10⁻⁶ M group, 2 nL for 10 × 10⁻⁶ M, and 6 nL for 100 × 10⁻⁶ M group) were printed, the droplets evaporate much faster than cell droplets. Therefore, to make all the conditions the same, the drugs need to be dried before transfection. After that, cells with or without transfection reagents were printed onto DMA by I-DOT One noncontact dispenser (Dispindex GmbH, Stuttgart, Germany) which is equipped with a powerful humidifier and a hygrometer. The humidity was set to 70% at 25 °C. As soon as humidity reached 70%, it started to print cells. After cell printing, the DMA slides were placed into a 10 cm petri dish with 3 mL of phosphate-buffered saline and a wet humidifying pads in the upper lid to prevent evaporation during incubation.

Screening Protocol: For the primary screening, the FDA-approved drug library was obtained in 10 × 10⁻³ M stock solution of DMSO and diluted with sterile water to produce 100 × 10⁻⁶ M prediluted plates. To do that, compounds were printed on 500 µm DMA. Then the DMA slides were dried in a desiccator under 50 mbar vacuum overnight. The positive control (drug-free) was set as gene transfection without any compound but in the presence of equivalent of DMSO. From the primary screening, 14 compounds were selected for validation and were prediluted as indicated for the primary screening. Validation was performed on 1 mm DMA and 384-well plate with the same protocol for primary screening, except cells on DMA were stained with Hoechst 33 342 to visualize cell nucleus and propidium iodide (PI) to distinguish dead cells. For confirmation, 4 compounds were picked and delivered in 96-well plates and tested in diverse parameters.

In Vitro Transfection: Transfection on 500 µm DMA: the 774 FDA-approved drugs were printed on the DMA at certain volumes and dried in the vacuum desiccator overnight. Complexes of GFP plasmid DNA and ScreenFectA transfection reagent were prepared with 0.3 µL ScreenFectA in 10 µL ScreenFect dilution buffer, followed by diluting a total of 300 ng GFP plasmid DNA in dilution buffer to a final volume of 10 µL. The two mixtures prepared above were then immediately mixed using rapidly slight pipette strokes and incubated for 20 min at room temperature for complex formation. After that, 80 µL fresh cell suspension at a concentration of 2 × 10⁶ cells mL⁻¹ were added to complexes and gently mixed with pipette. Then, the mixture was printed onto 500 µm DMA 20 nL per spot using I-DOT One Non-Contact Dispenser (Dispindex GmbH, Stuttgart, Germany) followed by a further 24 h incubation in the cell culture incubator. After that, formaldehyde solution was printed into each DMA spot to fix the cells before add immu-mount medium to mount cells on DMA followed by dried at 4 °C. Images of the individual spots were taken using the Olympus IX81 inverted motorized microscope (Olympus, Tokyo, Japan) and Keyence BZ-9000 microscope (KEYENCE, Osaka, Japan). Transfection efficiency was assessed after 24 h incubation. The transfection efficiency was quantified by counting the GFP positive cell numbers using Image J (<https://imagej.nih.gov/ij/>).

Transfection on 1 mm DMA: the transfection process was the same with the method described above. Briefly, the FDA-approved drugs were printed onto 1 mm DMA at certain volumes. Complexes of GFP plasmid DNA and ScreenFectA transfection reagent were prepared

with 0.15 μL ScreenFectA in 10 μL ScreenFect dilution buffer, followed by diluting a total of 150 ng GFP plasmid DNA in dilution buffer to a final volume of 10 μL . The two mixtures prepared above were then immediately mixed using rapidly slight pipette strokes and incubated for 20 min at room temperature for complex formation. After that, 80 μL fresh cell suspension at a concentration of 1.25×10^6 cells mL^{-1} were added to complexes and gently mixed with pipette. Then, the mixture was printed onto 1 mm DMA 100 nL per spot using I-DOT One Non-Contact Dispenser (Dispensix GmbH, Stuttgart, Germany) followed by a further 24 h incubation in the cell culture incubator. Then, 50 nL per spot of Hoechst 33 342 ($33.3 \mu\text{g mL}^{-1}$) and PI ($2.22 \mu\text{g mL}^{-1}$) solution was printed into each spot. The 1 mm DMA slide was placed into a standard 10 cm petri dish equipped with a humidifying pad to prevent evaporation for 15 min. Images of the individual spots were taken using the Olympus IX81 inverted motorized microscope (Olympus, Tokyo, Japan). The number of GFP positive, Hoechst 33 342 and PI positive cells were counted using Image J. Cell viability was calculated as the following equation: cell viability (%) = $1 - (\text{PI-positive cell numbers} / \text{Hoechst positive cell numbers}) \times 100$. The transfection efficiency was calculated as the following equation: transfection efficiency (%) = $(\text{GFP positive cell numbers} / \text{Hoechst positive cell numbers}) \times 100$.

Transfection in 384-well plate: The transfection process was the same as the method described above. Briefly, the FDA-approved drugs were pipetting into 384-well plates at certain volumes prior to overnight drying in the vacuum desiccator. Complexes of GFP plasmid DNA and ScreenFectA transfection reagent were prepared with 0.017 μL ScreenFectA in 10 μL ScreenFect dilution buffer, followed by diluting a total of 17 ng GFP plasmid DNA in dilution buffer to a final volume of 10 μL . The two mixtures prepared above were then immediately mixed using rapidly slight pipette strokes and incubated for 20 min at room temperature for complex formation. After that, 80 μL fresh cell suspension at a concentration of 7.13×10^4 cells mL^{-1} were added to complexes and gently mixed with pipette. Then, the mixture was manually seeding into each well at the volume of 20 μL followed by a further 24 h incubation in the cell culture incubator. Then, 2 μL per well Hoechst 33 342 ($100 \mu\text{g mL}^{-1}$) and PI ($6.67 \mu\text{g mL}^{-1}$) solution was added into each well and incubated for 15 min. Nine images of the individual well were taken using the Olympus IX81 inverted motorized microscope (Olympus, Tokyo, Japan). The number of GFP positive, Hoechst 33 342 and PI positive cells were counted using Image J. Cell viability was calculated as the following equation: cell viability (%) = $1 - (\text{PI-positive cell numbers} / \text{Hoechst positive cell numbers}) \times 100$. The transfection efficiency was calculated as the following equation: transfection efficiency (%) = $(\text{GFP positive cell numbers} / \text{Hoechst positive cell numbers}) \times 100$.

Transfection in 96-well plate: The transfection process was the same as the method described above. Briefly, the FDA-approved drugs were pipetting into 96-well plates at certain volumes prior to overnight drying in the vacuum desiccator. Complexes of GFP plasmid DNA and ScreenFectA transfection reagent were prepared with 0.1, 0.2, 0.3, and 0.4 μL ScreenFectA in 10 μL ScreenFect dilution buffer, respectively, followed by diluting a total of 50, 75, and 100 ng GFP plasmid DNA in dilution buffer to a final volume of 10 μL . The two mixtures prepared above were then immediately mixed using rapidly slight pipette strokes and incubated for 20 min at room temperature for complex formation. After that, 80 μL fresh cell suspension at a concentration of 3.75×10^5 cells mL^{-1} were added to complexes and gently mixed with pipette. Then, the mixture was manually seeding into each well at the volume of 100 μL followed by a further 24 h incubation in the cell culture incubator. Then, 10 μL per well Hoechst 33 342 ($100 \mu\text{g mL}^{-1}$) and PI ($6.67 \mu\text{g mL}^{-1}$) solution was added into each well and incubated for 15 min. 16 images of the individual well were taken using the Olympus IX81 inverted motorized microscope (Olympus, Tokyo, Japan). The number of GFP positive, Hoechst 33 342 and PI-positive cells were counted using Image J. Cell viability was calculated as the following equation: cell viability (%) = $1 - (\text{PI-positive cell numbers} / \text{Hoechst positive cell numbers}) \times 100$. The transfection efficiency was calculated as the following equation: transfection efficiency (%) = $(\text{GFP positive cell numbers} / \text{Hoechst positive cell numbers}) \times 100$.

Data Analysis and Statistics: Data were presented as mean \pm standard deviation (SD). The statistical significance of the experimental data were determined with a two-tailed Student *t*-test (p -value < 0.05) and the initial hits cut-off was set as control mean + 3SD.

Supporting Information

Supporting Information is available from the Wiley Online Library or from the author.

Acknowledgements

This research was supported by the ERC Starting Grant (ID: 337077-DropCellArray). The Chinese Scholarship Council (fellowship to Y.L.) is also gratefully acknowledged.

Conflict of Interest

The authors declare no conflict of interest.

Keywords

droplet microarrays, drugs, high-throughput screening, miniaturization, transfection

Received: October 31, 2019
Revised: December 4, 2019
Published online: February 11, 2020

- [1] a) G. Elliott, P. O'Hare, *Cell* **1997**, *88*, 223; b) J. H. Kim, Y. S. Kim, K. Park, E. Kang, S. Lee, H. Y. Nam, K. Kim, J. H. Park, D. Y. Chi, R. W. Park, I. S. Kim, K. Choi, I. Chan Kwon, *Biomaterials* **2008**, *29*, 1920; c) S. S. Bale, S. J. Kwon, D. A. Shah, A. Banerjee, J. S. Dordick, R. S. Kane, *ACS Nano* **2010**, *4*, 1493.
- [2] a) M. C. Morris, J. Depollier, J. Mery, F. Heitz, G. Divita, *Nat. Biotechnol.* **2001**, *19*, 1173; b) M. Kilpelainen, J. Riikonen, M. A. Vlasova, A. Huotari, V. P. Lehto, J. Salonen, K. H. Herzig, K. Jarvinen, *J. Controlled Release* **2009**, *137*, 166.
- [3] a) A. K. Salem, P. C. Searson, K. W. Leong, *Nat. Mater.* **2003**, *2*, 668; b) D. W. Pack, A. S. Hoffman, S. Pun, P. S. Stayton, *Nat. Rev. Drug Discovery* **2005**, *4*, 581.
- [4] D. Luo, W. M. Saltzman, *Nat. Biotechnol.* **2000**, *18*, 33.
- [5] T. G. Park, J. H. Jeong, S. W. Kim, *Adv. Drug Delivery Rev.* **2006**, *58*, 467.
- [6] C. M. Wiethoff, C. R. Middaugh, *J. Pharm. Sci.* **2003**, *92*, 203.
- [7] a) V. Labhasetwar, J. Bonadio, S. A. Goldstein, J. R. Levy, *Colloids Surf., B* **1999**, *16*, 281; b) S. Prabha, V. Labhasetwar, *Mol. Pharmaceutics* **2004**, *1*, 211.
- [8] a) J. Beloor, S. Ramakrishna, K. Nam, C. S. Choi, J. Kim, S. H. Kim, H. J. Cho, H. Shin, H. Kim, S. W. Kim, S. K. Lee, P. Kumar, *Small* **2015**, *11*, 2069; b) H. Y. Nam, K. Nam, H. J. Hahn, B. H. Kim, H. J. Lim, H. J. Kim, J. S. Choi, J. S. Park, *Biomaterials* **2009**, *30*, 665.
- [9] a) M. K. Gupta, S. H. Lee, S. W. Crowder, X. Wang, L. H. Hofmeister, C. E. Nelson, L. M. Bellan, C. L. Duvall, H. J. Sung, *J. Mater. Chem. B* **2015**, *3*, 7271; b) E. Yuba, Y. Kanda, Y. Yoshizaki, R. Teranishi, A. Harada, K. Sugiura, T. Izawa, J. Yamate, N. Sakaguchi, K. Koiwai, K. Mono, *Biomaterials* **2015**, *67*, 214.
- [10] a) J. A. Zuris, D. B. Thompson, Y. Shu, J. P. Guilinger, J. L. Bessen, J. H. Hu, M. L. Maeder, J. K. Joung, Z. Y. Chen, D. R. Liu,

- Nat. Biotechnol.* **2015**, *33*, 73; b) Y. Wang, A. Rajala, B. Cao, M. Ranjo-Bishop, M. P. Agbaga, C. Mao, R. V. Rajala, *Theranostics* **2016**, *6*, 1514.
- [11] a) H. X. Wang, Z. Song, Y. H. Lao, X. Xu, J. Gong, D. Cheng, S. Chakraborty, J. S. Park, M. Li, D. Huang, L. Yin, J. Cheng, K. W. Leong, *Proc. Natl. Acad. Sci. USA* **2018**, *115*, 4903; b) L. Liu, H. Yi, H. He, H. Pan, L. Cai, Y. Ma, *Biomaterials* **2017**, *134*, 166.
- [12] D. Putnam, *Nat. Mater.* **2006**, *5*, 439.
- [13] a) S. D. Patil, D. G. Rhodes, D. J. Burgess, *AAPS J.* **2005**, *7*, E61; b) H. Lv, S. Zhang, B. Wang, S. Cui, J. Yan, *J. Controlled Release* **2006**, *114*, 100.
- [14] H. Luthman, G. Magnusson, *Nucleic Acids Res.* **1983**, *11*, 1295.
- [15] S. Napoli, G. M. Carbone, C. V. Catapano, N. Shaw, D. P. Arya, *Bioorg. Med. Chem. Lett.* **2005**, *15*, 3467.
- [16] J. S. Choi, K. S. Ko, J. S. Park, Y. H. Kim, S. W. Kim, M. Lee, *Int. J. Pharm.* **2006**, *320*, 171.
- [17] D. Li, P. Li, G. Li, J. Wang, E. Wang, *Biomaterials* **2009**, *30*, 1382.
- [18] A. K. Becker, H. Erfle, M. Gunkel, N. Beil, L. Kaderali, V. Starkuviene, *High-Throughput* **2018**, *7*, 13.
- [19] a) G. Arrabito, C. Galati, S. Castellano, B. Pignataro, *Lab Chip* **2013**, *13*, 68; b) G. Arrabito, F. Cavaleri, V. Montalbano, V. Vetri, M. Leone, B. Pignataro, *Lab Chip* **2016**, *16*, 4666.
- [20] a) S. P. Zhao, Y. Ma, Q. Lou, H. Zhu, B. Yang, Q. Fang, *Anal. Chem.* **2017**, *89*, 10153; b) Y. L. Chen, D. Gao, Y. W. Wang, S. Lin, Y. Y. Jiang, *Anal. Chim. Acta* **2018**, *1036*, 97; c) Z. H. Wang, M. C. Kim, M. Marquez, T. Thorsen, *Lab Chip* **2007**, *7*, 740.
- [21] a) D. B. Wheeler, S. N. Bailey, D. A. Guertin, A. E. Carpenter, C. O. Higgins, D. M. Sabatini, *Nat. Methods* **2004**, *1*, 127; b) J. M. Silva, H. Mizuno, A. Brady, R. Lucito, G. J. Hannon, *Proc. Natl. Acad. Sci. USA* **2004**, *101*, 6548; c) B. Neumann, M. Held, U. Liebel, H. Erfle, P. Rogers, R. Pepperkok, J. Ellenberg, *Nat. Methods* **2006**, *3*, 385.
- [22] Y. Zhu, L. N. Zhu, R. Guo, H. J. Cui, S. Ye, Q. Fang, *Sci. Rep.* **2015**, *4*, 5046.
- [23] W. Q. Feng, L. X. Li, E. Ueda, J. S. Li, S. Heissler, A. Welle, O. Trapp, P. A. Levkin, *Adv. Mater. Interfaces* **2014**, *1*, 1400269.
- [24] a) E. Ueda, F. L. Geyer, V. Nedashkivska, P. A. Levkin, *Lab Chip* **2012**, *12*, 5218; b) T. Tronser, A. A. Popova, M. Jaggy, M. Bastmeyer, P. A. Levkin, *Adv. Healthcare Mater.* **2017**, *6*, 1700622; c) G. E. Jogia, T. Tronser, A. A. Popova, P. A. Levkin, *Microarrays* **2016**, *5*, 28; d) A. A. Popova, S. M. Schillo, K. Demir, E. Ueda, A. Nesterov-Mueller, P. A. Levkin, *Adv. Mater.* **2015**, *27*, 5217; e) T. Tronser, K. Demir, M. Reischl, M. Bastmeyer, P. A. Levkin, *Lab Chip* **2018**, *18*, 2257; f) A. A. Popova, T. Tronser, K. Demir, P. Haitz, K. Kuodyte, V. Starkuviene, P. Wajda, P. A. Levkin, *Small* **2019**, *15*, 1901299.
- [25] S. Obayashi, K. Deb, C. Poloni, T. Hiroyasu, T. Murata, *Evolutionary Multi-Criterion Optimization*, Springer, Matsushima, Japan **2007**.
- [26] a) S. Basiouni, H. Fuhrmann, J. Schumann, *BioTechniques* **2012**, *53*, 1; b) W. P. R. Verdurmen, R. Wallbrecher, S. Schmidt, J. Eilander, P. Bovee-Geurts, S. Fanghänel, J. Bürck, P. Wadhvani, A. S. Ulrich, R. Brock, *J. Controlled Release* **2013**, *170*, 83; c) B. Fadnes, A. Husebekk, G. Svineng, O. Rekdal, M. Yanagishita, S. O. Kolset, L. Uhlin-Hansen, *Glycoconjugate J.* **2012**, *29*, 513.
- [27] R. Z. Wu, S. N. Bailey, D. M. Sabatini, *Trends Cell Biol.* **2002**, *12*, 485.
- [28] a) M. Yoshimura, T. Oka, *Proc. Natl. Acad. Sci. USA* **1990**, *87*, 3670; b) H. J. Yeh, M. Chrzanowska, A. Brossi, *FEBS Lett.* **1988**, *229*, 82; c) J. M. Lehmann, J. M. Lenhard, B. B. Oliver, G. M. Ringold, S. A. Kliewer, *J. Biol. Chem.* **1997**, *272*, 3406.